AFWL-TR-75-261

Theoretical Notes
Note 274

AFWL-TR-
75-261

TN 274

# A THREE-DIMENSIONAL SYSTEMS GENERATED ELECTROMAGNETIC PULSE CALCULATION OF AN IDEALIZED FLTSATCOM SATELLITE

B. Goplen, et al.

Science Applications, Inc.
122 La Veta, NE
Albuquerque, New Mexico 87108

June 1976

Final Report



AIR FORCE WEAPONS LABORATORY
Air Force Systems Command
Kirtland Air Force Base, NM 87117

UNCLASSIFIED

SECURITY CLASSIFICATION OF THIS PAGE *(When Data Entered)*

## REPORT DOCUMENTATION PAGE

READ INSTRUCTIONS BEFORE COMPLETING FORM

| | |
|---|---|
| 1. REPORT NUMBER: AFWL-TR-75-261 | 2. GOVT ACCESSION NO. |
| 3. RECIPIENT'S CATALOG NUMBER | |
| 4. TITLE *(and Subtitle)*: A THREE-DIMENSIONAL SYSTEMS GENERATED ELECTRO-MAGNETIC PULSE CALCULATION OF AN IDEALIZED FLTSATCOM SATELLITE | 5. TYPE OF REPORT & PERIOD COVERED: Final Report |
| | 6. PERFORMING ORG. REPORT NUMBER: SAI-75-512-A0 |
| 7. AUTHOR(s): B. Goplen, J. E. Morel, O. Lopez, W. A. Seidler, R. E. Clark | 8. CONTRACT OR GRANT NUMBER(s): F29601-74-C-0124 |
| 9. PERFORMING ORGANIZATION NAME AND ADDRESS: Science Applications, Inc. 122 La Veta, NE Albuquerque, NM 87108 | 10. PROGRAM ELEMENT, PROJECT, TASK AREA & WORK UNIT NUMBERS: 64711F, 4695 WDNE0709 |
| 11. CONTROLLING OFFICE NAME AND ADDRESS: Air Force Weapons Laboratory (ELP) Kirtland Air Force Base, NM 87117 | 12. REPORT DATE: June 1976 |
| | 13. NUMBER OF PAGES |
| 14. MONITORING AGENCY NAME & ADDRESS *(if different from Controlling Office)* | 15. SECURITY CLASS. *(of this report)*: UNCLASSIFIED |
| | 15a. DECLASSIFICATION/DOWNGRADING SCHEDULE |

16. DISTRIBUTION STATEMENT *(of this Report)*

Approved for public release; distribution unlimited.

17. DISTRIBUTION STATEMENT *(of the abstract entered in Block 20, if different from Report)*

18. SUPPLEMENTARY NOTES

19. KEY WORDS *(Continue on reverse side if necessary and identify by block number)*

System Generated Electromagnetic Pulse (SGEMP)
Satellite System Analysis
SGEMP Prediction Technique

20. ABSTRACT *(Continue on reverse side if necessary and identify by block number)*

A three-dimensional systems generated electromagnetic pulse (SGEMP) code, MAD3, has been written to calculate replacement currents on structures subjected to X-radiation. Initial results are presented for calculated boom currents on an idealized FLTSATCOM satellite. These results were obtained using a fully dynamic and self-consistent solution of Maxwell's equations at a low fluence level. Modifications are presently being made to the MAD3 code to permit treatment of cases involving space-charge limiting.

DD FORM 1 JAN 73 1473 EDITION OF 1 NOV 65 IS OBSOLETE

SECURITY CLASSIFICATION OF THIS PAGE *(When Data Entered)*

## SUMMARY

A series of one-, two-, and three-dimensional SGEMP codes have been developed and applied to an asymmetric calculation of skin currents on an idealized FLTSATCOM satellite. The techniques employ a second order center differing of the dynamic Maxwell equations and a Birdsall cloud-in-cell treatment of the electron plasma. The results of these treatments is a believable calculation of the currents flowing on the FLTSATCOM solar panel booms. The current frequency agrees well with that obtained from a circuit analog model[10]. The peak value for boom currents is 100 amperes.

TABLE OF CONTENTS

LIST OF FIGURES

# SECTION I

# INTRODUCTION

This report discusses first results obtained from a three-dimensional calculation of skin currents induced by systems generated electromagnetic pulse (SGEMP) on an idealized FLTSATCOM. A drawing of the FLTSATCOM satellite is shown in Figure 1. From a calculational standpoint, this structure is extremely complex, having surfaces of varying shapes and orientations, external antenna systems, thin structural members, and a very complicated interior structure. Even neglecting the question of coupling to critical interior circuits, the SGEMP problem appears formidable. The objective of this work is the development of calculational techniques which take into account the three-dimensional nature and a reasonable amount of the structural detail found in real satellites. Initial results are presented for current on the boom connecting the solar panels to the main body of the satellite.

SGEMP on a system in vacuum results from interaction of incident photons with the structure itself. The x-ray pulse gives rise to surface emission of low-energy electrons, which provide a current, or driving function, for electromagnetic fields in accord with predictions of Maxwell's equations. At high fluence levels, the resulting higher fields can substantially alter electron trajectories, thus necessitating self-consistent calculations in which the currents driving the electromagnetic fields are also affected by them. In one extreme form, this manifests itself in the phenomenon known as space-charge limiting. Thus, a large electric field component normal to an emitting surface can rapidly draw lower energy electrons back into the surface in very short distances and periods of time. These low-energy electrons form a sheath, or boundary layer, the characteristics of which dominate the transmission of higher energy components which continue to drive the electromagnetic fields.

In addition to difficulties imposed by space-charge limiting, there are many other problems associated with performing meaningful calculations for real systems. Circuit responses are due to effects commonly divided by origin into two classes: 1) radiation on the interior of cables, and 2) external replacement (or skin) currents. To consider this second problem, Science Applications, Inc. (SAI) has, during a five month period, created a

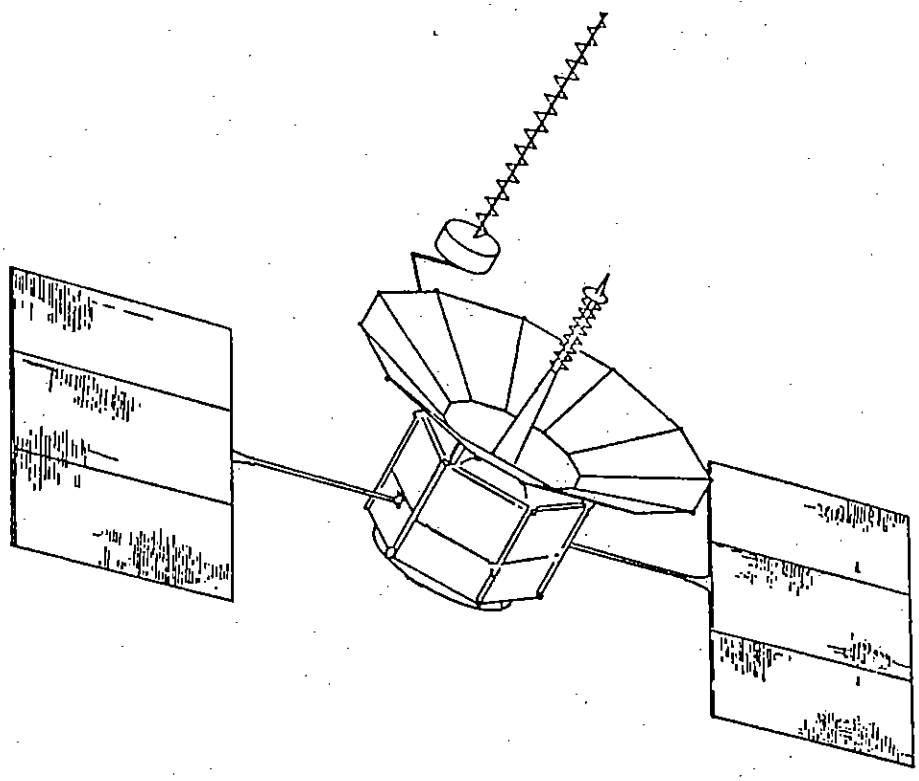

Figure 1. Drawing of a FLTSATCOM

series of one-, two-, and three-dimensional SGEMP codes, known as the MAD codes. The general approach taken has been to verify methods and techniques in one or two dimensions before incorporating them into the three-dimensional calculation. This report briefly describes some initial results obtained from a three-dimensional calculation of an idealized FLTSATCOM satellite using the MAD3 code.

# SECTION I

# THE MAD3 CODE

The MAD3 code is a union of the particle pusher algorithm, MUST,[1] and the electromagnetic fields algorithm, A3D.[2] This code was created expressly to provide the capability to perform three-dimensional SGEMP calculations. This section is intended to provide an overview of the salient features of the calculation.

## 1. Solution of Maxwell's Equations

The fields algorithm in MAD3 is, at present, a fully dynamic treatment of Maxwell's equations in three spatial dimensions and time. The grid spacing is chosen to provide second-order accuracy in the numerical differencing scheme, both in space and time. Figure 2 illustrates the definition of fields associated with the unit cell in the spatial coordinates. Use is made of the metric tensor in writing the differential equations; the resulting difference equations are applicable to any locally orthogonal coordinate system. Provision is also made for nonuniform spacing either functionally or arbitrarily to permit better accuracy near structural elements and at the same time provide separation from a free-space boundary. The usual limitation upon allowable time step size is provided by the Courant stability criterion.

Boundary conditions for metals are imposed by choosing spacing so that the tangential electric fields are defined to lie on structural surfaces. These tangential fields must vanish for a perfect conductor. Since the time spacing of the electric and magnetic fields is defined to differ by $\delta t/2$, it is possible to ignore structure in calculating electrical fields. The correct boundary condition must be set before the magnetic field calculation. By this means problems of multiple do-loops or if-statements associated with structure are eliminated.

Additional boundary conditions are required for fields at the lower and upper limits of the three spatial coordinates. For the idealized FLTSATCOM being considered, two orientations ($\theta = 0, \pi/2$) of the solar panels are possible which preserve mirror symmetry. For

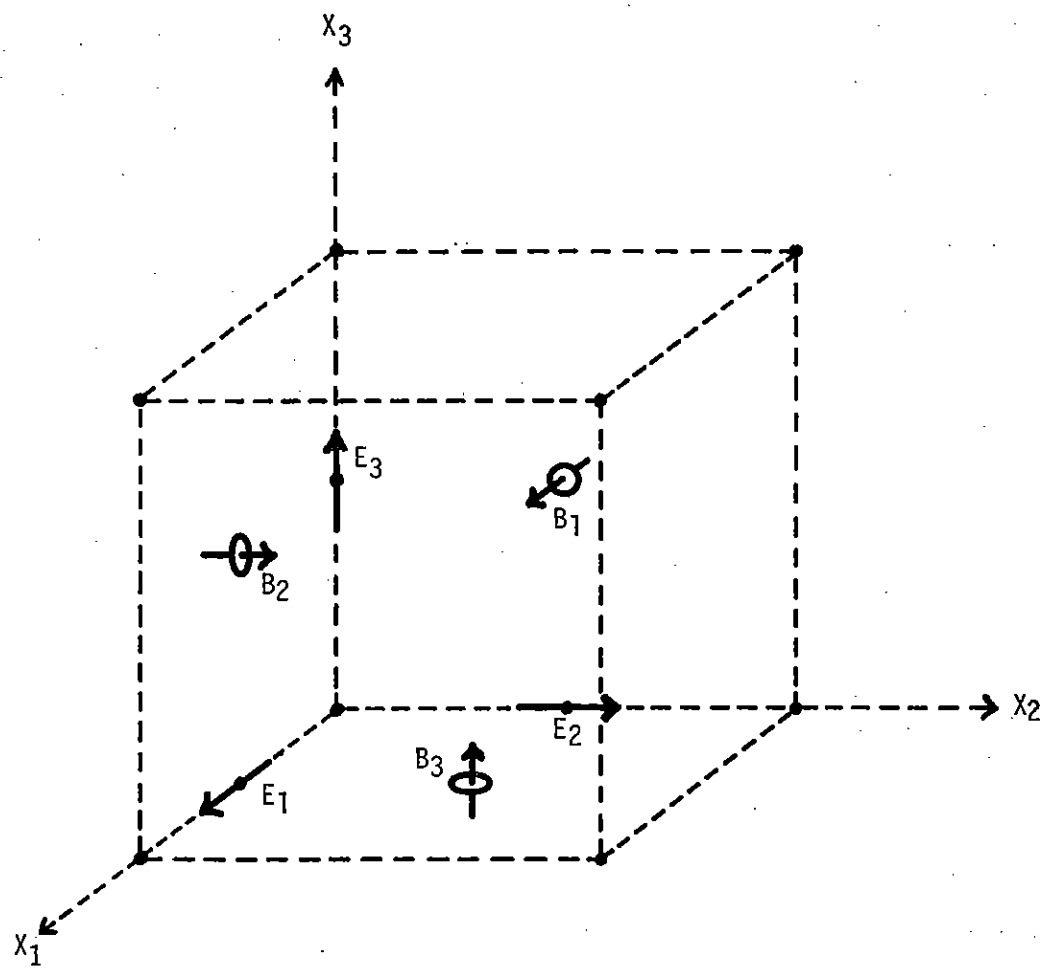


Figure 2. Definition of Field Locations in the Spatial Coordinates

the side-on orientation, the required boundary condition is that the odd-parity fields ($E_\theta$, $B_r$, and $B_z$) must vanish at $\theta = 0$ and $\theta = \pi$. This condition is obtained by choosing spacing such that these fields are defined at the proper locations.

The inner boundary ($r = 0$) condition is obtained by choosing the axial electric field component ($E_z$) to be defined on the axis, and applying Stokes' theorem. The line integral of the magnetic field and area integral of current are numerically similar to the general differencing algorithm, so that the Stokes' theorem result can be obtained directly, and requires only averaging.

At the outside of the calculational grid ($z = z_{min}$, $z = z_{max}$, and $r = r_{max}$), the desired boundary condition should represent the propagation of a wave into free space. For this purpose a radiation boundary condition[3] has been implemented. This involves an interpolation of retarded time transverse fields at an inner point to obtain the correct functional form, and also includes geometrical considerations in setting the outermost fields. Complete freedom is allowed in the angular dependence, as opposed to the more correct approach of forcing this dependence to a functional form.[4] However, the radiation boundary condition has been found to allow significant reduction in the size of outer boundaries without affecting measurements at the satellite structure.

## 2. The Particle Pusher

The MUST particle pusher algorithm makes use of techniques developed by Boris[5]. This scheme involves use of a local Cartesian coordinate system to calculate particle motion. At present, the MAD3 particle pusher is written in cylindrical coordinates; however, use of the local Cartesian system will permit generalization to an arbitrary coordinate system.

The differencing scheme in the temporal coordinate is second-order. Fields and particle coordinates are defined in time as shown in Figure 3. As discussed previously, the time step for the fields calculation ($\delta t$) is limited in size by a stability criterion. The time step used for pushing particles is limited by the requirement that particles travel less than one cell width in a time step. Therefore, the particle time step ($N\delta t$) can generally be made some odd multiple of the fields time step. This is illustrated in Figure 3 using the value, N = 3. Figure 3 also shows the leapfrog (centered difference) scheme for the electric and magnetic fields. To calculate forces on the particle, the magnetic field must be advanced half a time step ($\delta t/2$) to coincide with the electric fields and the particle position at time $k\delta t$. Momentum, and thus velocity, is then advanced from $(k-3/2)\delta t$ to $(k+3/2)\delta t$. A second-order integration yields the new particle positions at time $(k+3)\delta t$. The new values of velocity and average particle position are used to calculate the current source, J. Following advancement of the magnetic fields by $\delta t/2$, the usual leapfrog scheme is used to calculate electric and magnetic fields until the next particle push. During this time, the source current, J, does not change. Computer running time is usually dominated by the particle calculations; this is a primary consideration in choosing the time step to be as large as possible for the particle motion.

An example of the local Cartesian frame used to calculate particle trajectories is shown in Figure 4. In this two-dimensional example, the original particle position vector, $\bar{r}$, is used to define a local Cartesian frame $(\hat{r},\hat{\theta})$. The particle motion is then calculated relative to these orthogonal unit vectors. Calculation of the new particle coordinates, $r'$ and $\theta'$, involves both a square root and an arctangent

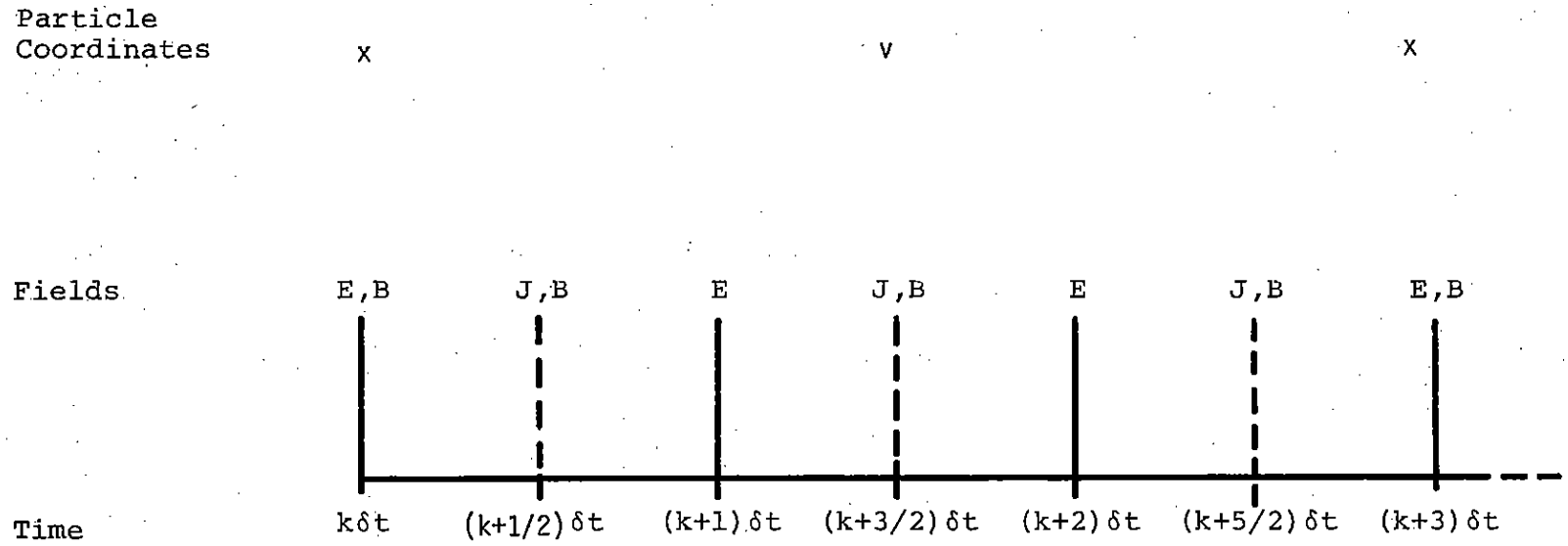


Figure 3. Definition of Fields and Particle Coordinates in Time

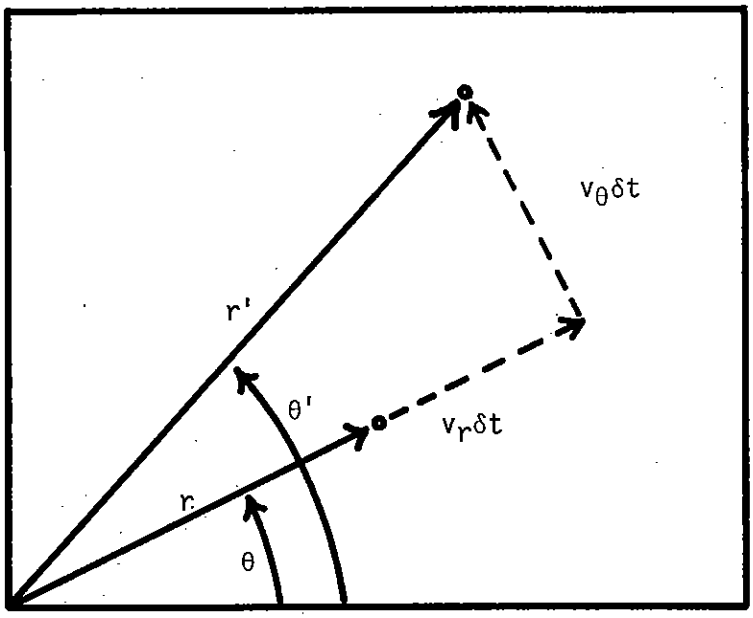


Figure 4. Local Cartesian Frame for Particle Motion

calculation. However, problems involving singularities and angular momentum conservation are avoided. Furthermore, the local Cartesian frame concept can be generalized to any arbitrary orthogonal coordinate system, although transformations become generally complex. Thus, use of this method offers the promise of a particle pusher algorithm suitable for generalized coordinates. As has been stated, the fields algorithm is already written in generalized coordinates.

Particles used in the MAD3 code, of course, represent very large numbers of electrons. At present, we are using particles of finite size and uniform density. These particles are assumed to deform to the size and orientation of the unit cell where they are located, and thus do not retain original dimensions. Considerations of uniform density are taken into account in performing area-weighting interpolations. Such interpolations are necessary to determine the fields used to push particles as well as the particle contributions to current sources.

The treatment of particles at outer and inner boundaries of the calculation should also be discussed. At the outer boundaries, a particle is simply allowed to disappear after it no longer contributes to the current source at $i_{max} - 1$. This method works because the radiation boundary condition is used for setting electric fields at the outer boundary. However, there is no mechanism for electrons to return into the calculation once they are lost.

A more difficult problem is the treatment of particles on the inner boundary (r=o). Briefly stated, the scheme for allocating a particle's contribution to 24 source terms breaks down as the origin is approached, and a transition must be made to a scheme which allows contribution to the multiply-defined sources near the origin. A prescription using radial weighting has been found which allows the desired transition while maintaining the symmetry properties of the current field.

## SECTION III

## ELECTRON EMISSION

In SGEMP, incident photons from a nuclear burst interact with the structure of a system, giving rise to a large flux of surface-emitted electrons. The interaction of incident photons with structure and the electron transport problem may be treated by several methods. These include an analytic approach, as embodied in QUICKE2[6], and the Monte Carlo calculation in POEM[7]. Both of these codes have been used to generate surface electron emission data for the FLTSATCOM calculations. Examples will be presented of POEM code results for a 5 keV blackbody spectrum.

The electron emission is, in general, a function of the energy spectrum, time history, and angle of incidence ($\theta_i$) of the incident photons, as well as the polar angle ($\theta$), azimuthal angle ($\phi$), and energy (E) of the emitted electrons. Figure 5 illustrates the definition of these variables in the local (surface) coordinate frame. The surface emission spectrum is generally a correlated function of the above variables. For these calculations, we have assumed that the incident photons can be described by a separable product function in energy and time. Further, the electron emission spectrum is usually uncoupled in energy and incident photon angle. Some degree of correlation exists between the polar and azimuthal angular distributions. This azimuthal asymmetry has recently been calculated[8] as a function of photon angle of incidence and energy. The extent of asymmetry diminishes substantially with decreasing photon energy. Further, recent two-dimensional calculations[9] suggest that the emission asymmetry may not be an important SGEMP effect. Therefore, for low-energy x-rays, the electron emission spectrum can be treated as a product function in all variables.

The electron energy spectrum from one-dimensional POEM code calculations is shown in Figure 6. The incident photon spectrum is 5 keV black body. The polar angle distribution for forward emission is shown in Figure 7, and is seen to approach very closely a cos $\theta$ distribution. The electron yield is a fairly weak function of incident photon angle, as indicated in Figure 8.

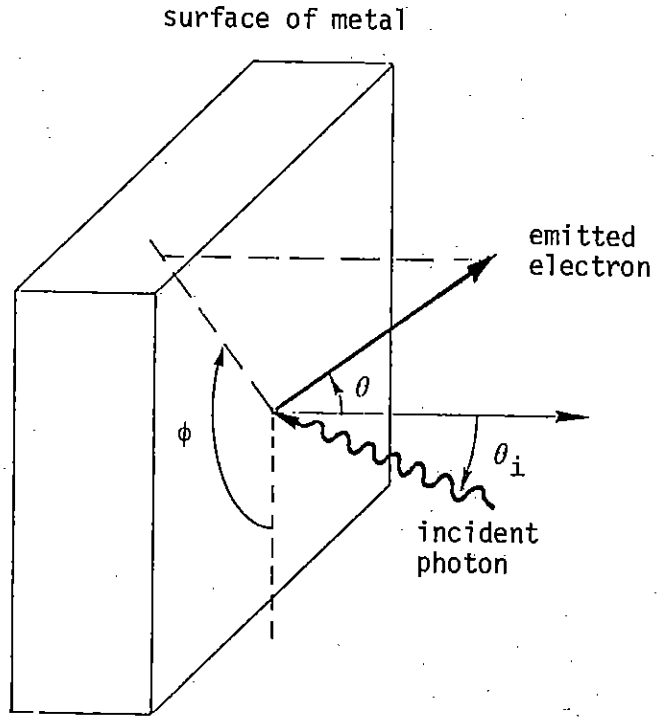


Figure 5. Local Coordinate System for Surface Emission

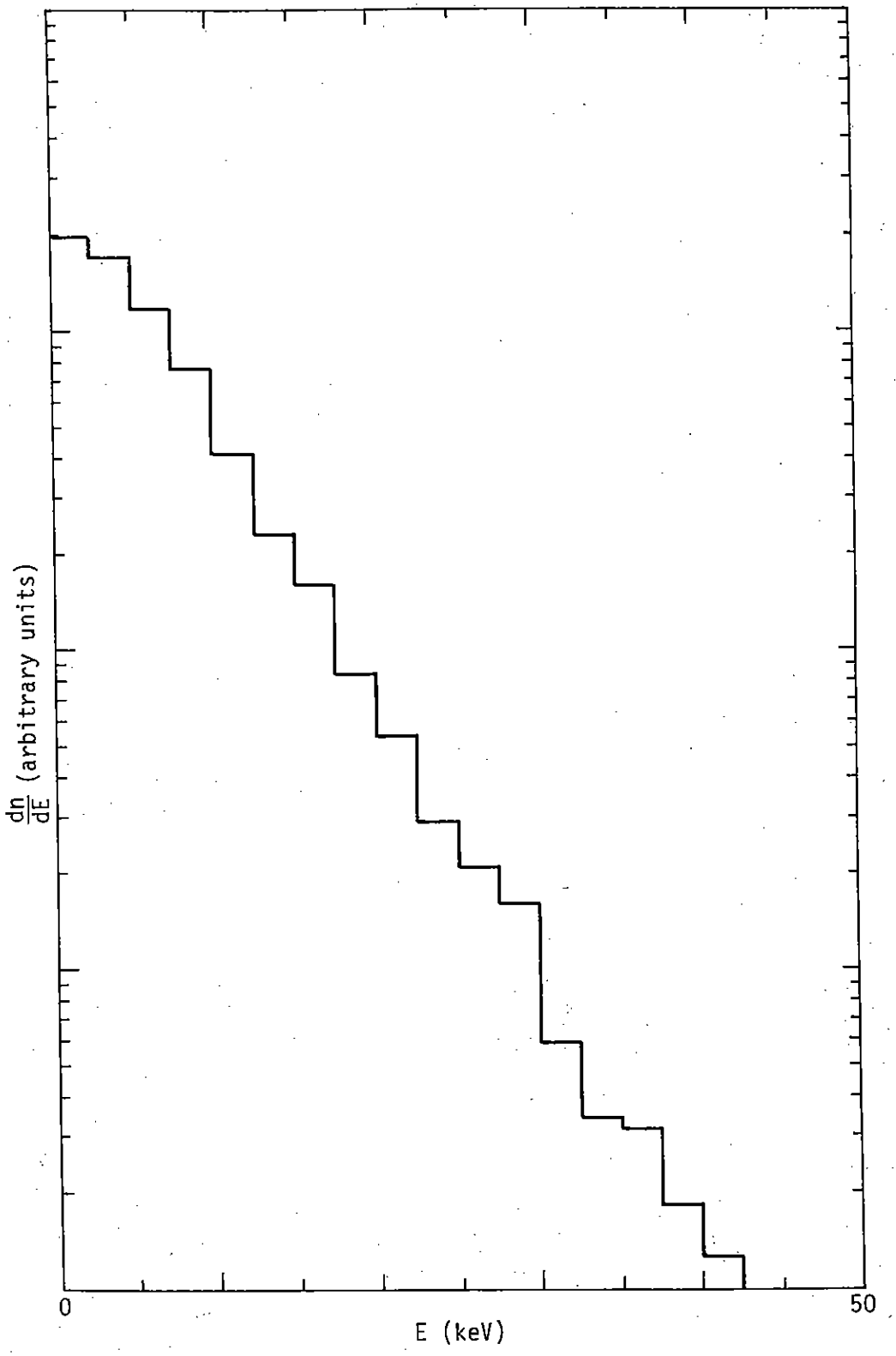


Figure 6. Electron Energy Spectrum

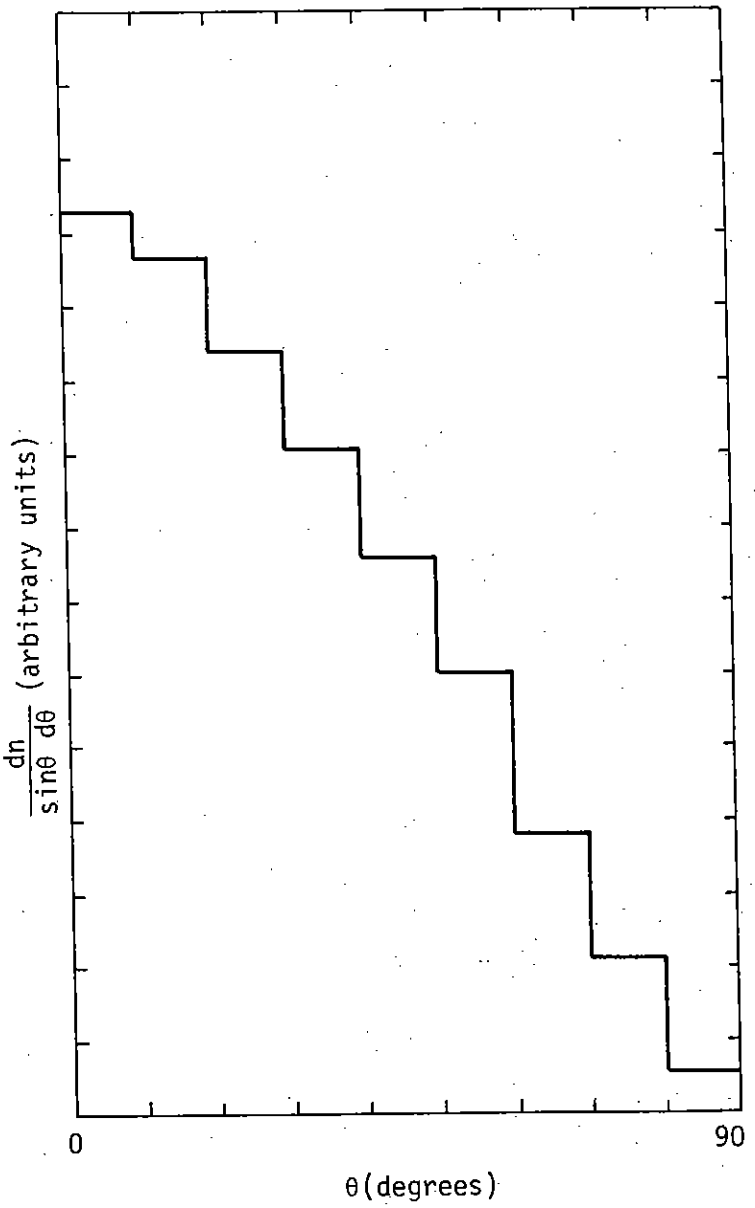


Figure 7. Electron Polar Angle Distribution for Forward Scattering

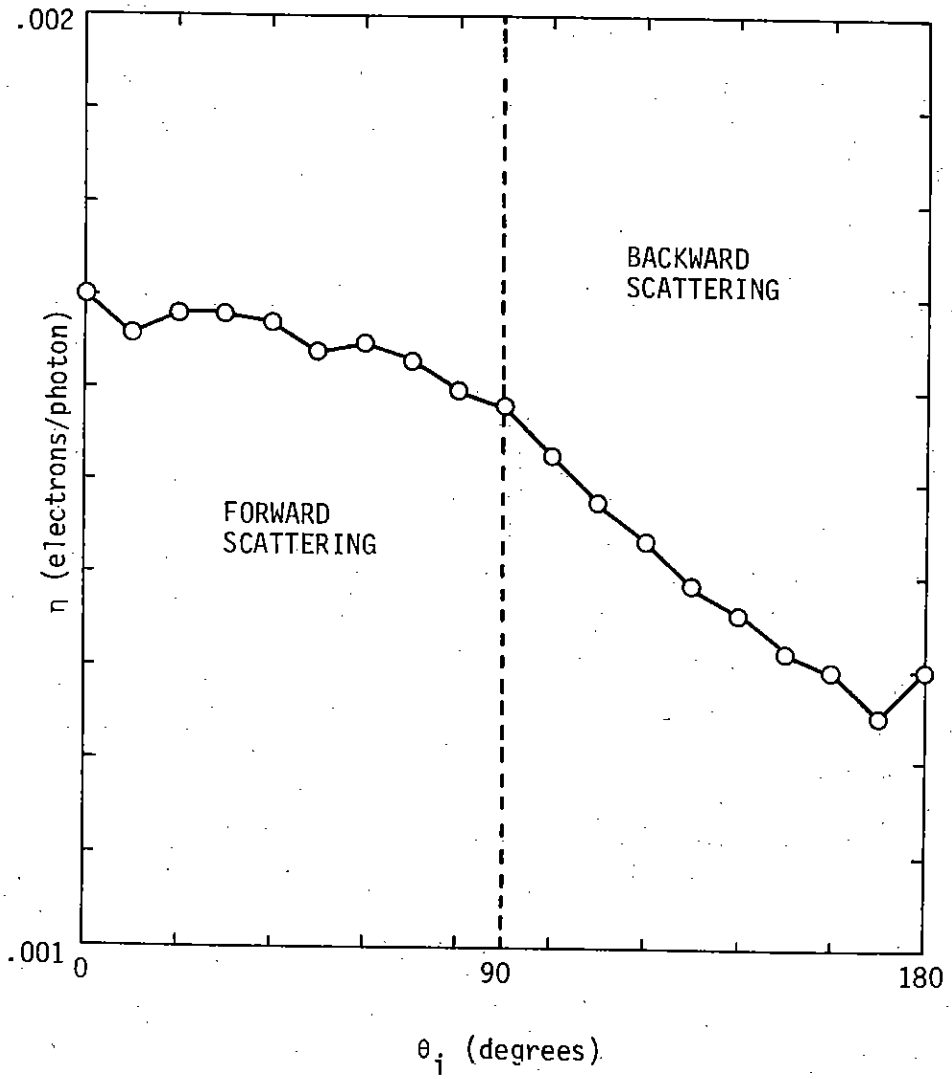


Figure 8. Electron Yield vs. Incident Photon Angle

## SECTION IV

## CALCULATED RESULTS FOR AN IDEALIZED FLTSATCOM SATELLITE

As a first step in furthering our ability to perform meaningful SGEMP calculations for systems of interest, the MAD3 code was set up to calculate the response of an idealized FLTSATCOM satellite. This model consists of a can, open on one end and closed on the other, which is joined to solar panels by thin arms, or booms. This model of an idealized FLTSATCOM is shown in Figure 9.

There are two cases of symmetry available using the model shown in Figure 9. The solar panels can be oriented either at $0^{o}$ (edgewise) or at $90^{o}$ (side-on) to the incident x-ray pulse. For these calculations, we chose the second case, in which the solar panels are directly exposed to the incident radiation. Symmetry then allows limiting the calculation in azimuthal angle, according to $0 \leq \theta \leq \pi$. The angle of burst measured from the vertical axis of the satellite ($\gamma$) remains arbitrary; calculations were performed for $\gamma$ values of 0, 60, 120, and 180 degrees.

Electron surface emission was allowed to occur from all surfaces of the satellite, including the main body (interior and exterior) and both sides of the solar panels. These structures were considered infinitesimally thin with respect to x-ray absorption, although geometrical factors can easily be used to account for attenuation of the photon flux. The orientation of the incident photons with respect to the vertical axis was made arbitrary, and calculations were performed at several polar angles. This factor, along with the curved surface of the main body, introduces variation in the photon angle of incidence ($\theta_i$) in the local (surface) coordinate system. This necessitates a transformation for momentum components generated in the local coordinate system to the satellite coordinate system. This transformation requires two matrix multiplications, but is simplified somewhat because one coordinate is always normal to metallic surfaces in our arbitrary orthogonal coordinate system. For these calculations, the particle injection scheme required random sampling, using 10 bins in energy, 9 in polar angle, and 36 in azimuthal angle of the local coordinate system. Eight particles were injected at each surface cell-time step, resulting in over $10^{5}$ particles in the system at maximum.

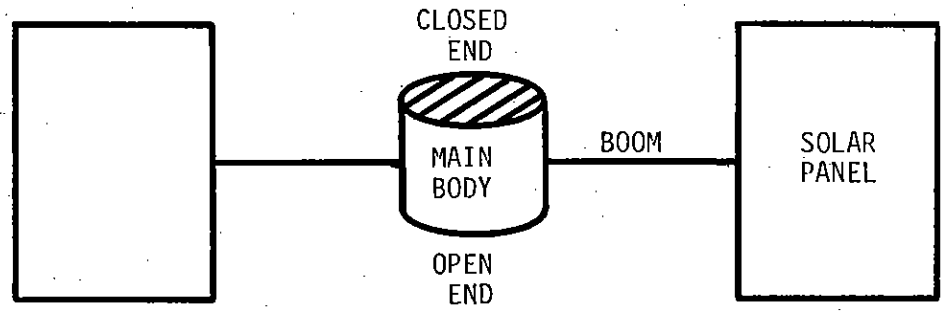


Figure 9. Model of an Idealized FLTSATCOM Satellite

The grid spacing for differencing the electromagnetic fields consisted of 20 spaces in the radial coordinate, 9 in the theta coordinate, and 24 in the axial coordinate. In addition, nonuniform spacing was used in the radial and axial coordinates to provide maximum separation between structure and outer boundaries, and finer spacing adjacent and normal to metallic surfaces.

Despite liberties taken with the grid, the spacing remains too coarse to correctly simulate very thin metallic structures, such as solar panels, with the usual technique. Because of this problem, it was hypothesized that a reasonable approximation to such structures could be obtained by forcing only those electric fields defined in the plane to vanish. This prescription was carried to its extreme in modeling the boom connecting the main body and solar panels by zeroing a single line of (radial) electric field components. Total skin currents on the boom can then be obtained from a numerical line integral of the magnetic field.

It is clear, at least, that this technique provides a mechanism for simulating electron flow on very thin structures. An investigation is presently being made of the accuracy of the model; however, it is expected to provide order-of-magnitude results. Previously, two-dimensional calculations were performed in which the boom radius was made increasingly small. These results, along with a three-dimensional Cartesian simulation, will allow better insight to the validity of this technique.

Figure 10 shows electric field components in a plane which passes through the solar panels. The magnitude of the field in decades is represented by the length of the arrow. This frame occurred after the source peak, and was selected from a motion picture sequence. Only the right half of this picture represents calculated results, while the left half is obtained from symmetry.

The calculation was performed at a fluence level of $10^{-3}$ cal/cm$^2$, with the photons incident at an angle of $60^{\circ}$ from the vertical axis of the satellite.

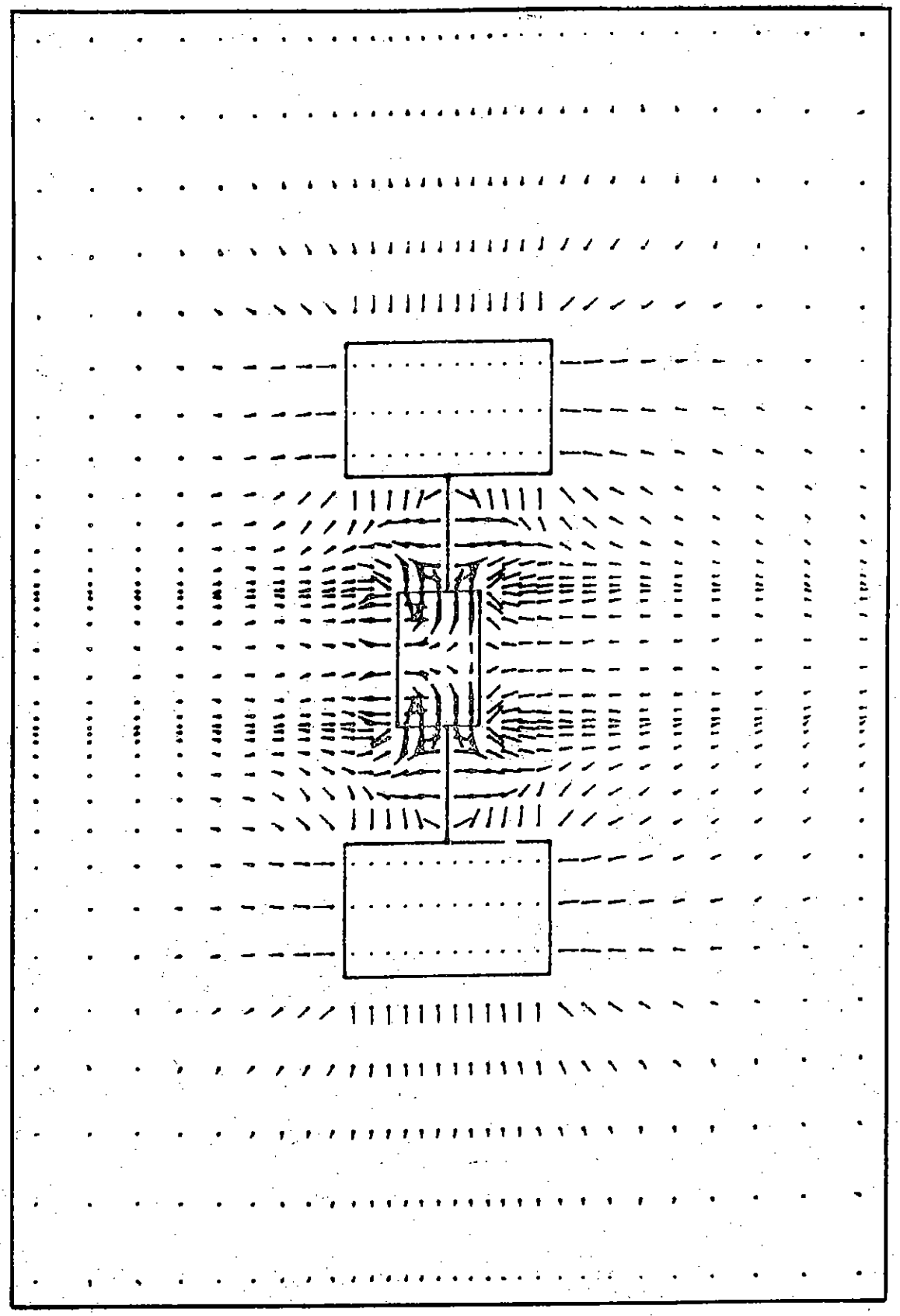

Figure 10. Electric Fields in a Plane through the Solar Panels

A plot of the skin current on the solar panel boom is shown in Figure 11. The plot uses a logarithmic scale for current, and a dashed line represents a negative value. The boom current is seen to oscillate in time, with a frequency which can be related to the characteristic dimensions of the FLTSATCOM configuration.

This frequency agrees fairly well with that obtained from a circuit analog model[10]. Comparisons have also been made with the two-dimensional results of Mangan and Perala[11]. Frequency responses seem to be similar; the difference has been ascribed to excitation of a three-dimensional mode, while the two-dimensional calculation was dominated by reflection between adjacent flat surfaces. Results have also been compared with those of Marin, et al[12], who used an integral equation formulation to calculate boom currents. However, the magnitude of their calculated current seems too large to be credible. The peak value for boom currents shown in Figure 11 is about 100 amperes.

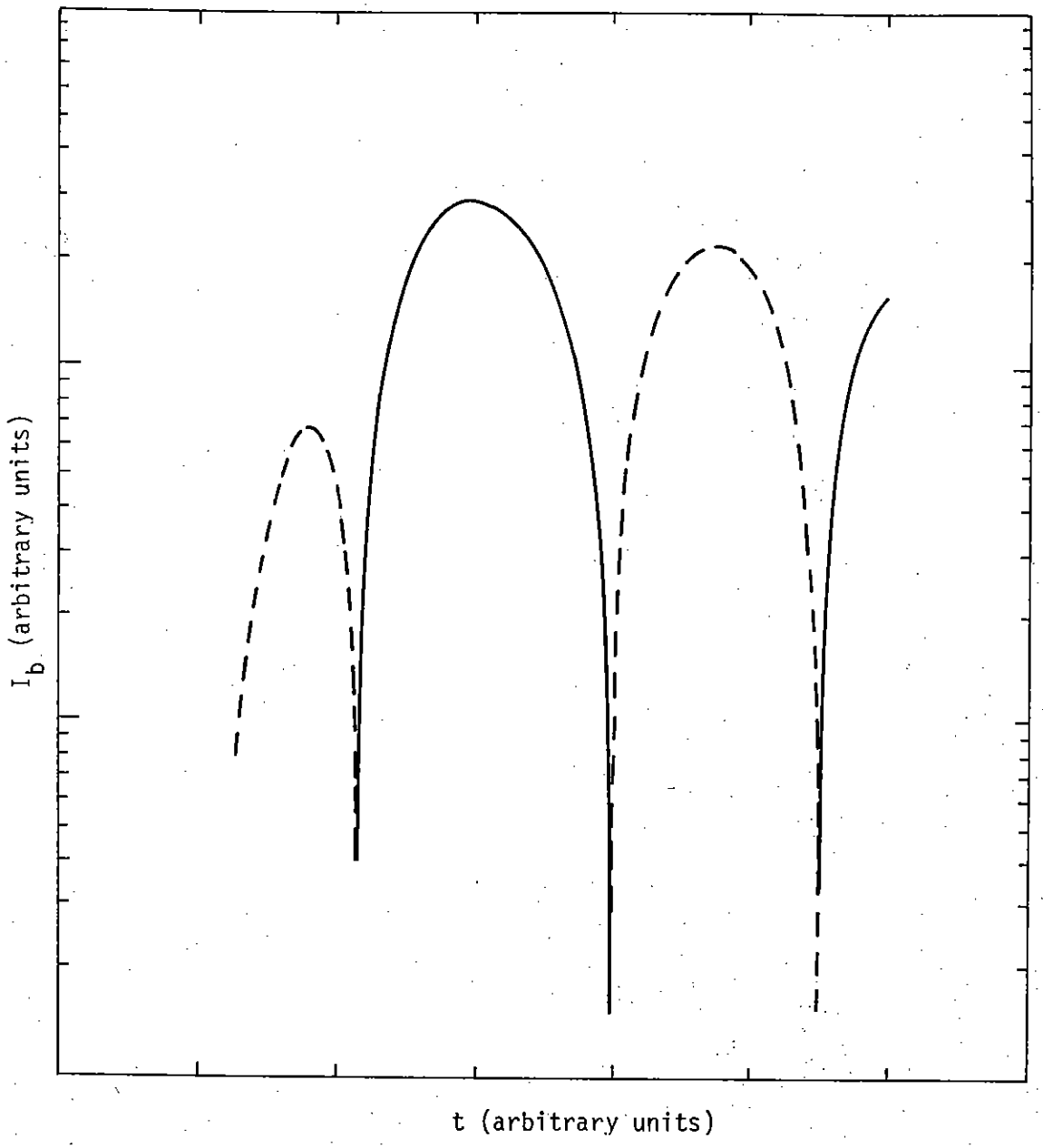


Figure 11. Skin Current on the Solar Panel Boom of an Idealized FLTSATCOM Satellite

## SECTION V

## PRESENT STATUS OF CALCULATIONS AND WORK IN PROGRESS

This document is intended to illustrate the present capability to perform meaningful SGEMP analyses for complex satellite structures. This section briefly describes work now underway to extend this capability.

The techniques used to model very thin structures are of obvious importance in being able to describe complex structural details. These techniques are exemplified in extreme form by the model of the boom which joins solar panels to the main body of the FLTSATCOM. A study is currently being done to assess the adequacy of this model. First, two-dimensional calculations, if possible analytical, are being performed for the case of specified Compton current moving externally along an infinitely long wire of fixed radius. Second, this same physical problem is being modeled with the three-dimensional code, LAD3 (a nonself-consistent version of MAD3) in Cartesian coordinates. (Cartesian coordinates most closely simulate the actual differencing scheme at the boom in the FLTSATCOM calculations.) In the three-dimensional calculation, the wire will be modeled by a single line of vanishing (z-component) electric fields. Comparison with the exact two-dimensional calculations will allow assessment of the accuracy of this technique as a function of wire diameter and three-dimensional grid spacing.

Another area requiring effort is the development of an arbitrary coordinate system for the particle pusher. As has already been stated, the MAD3 fields algorithm makes use of an arbitrary orthogonal system, while the particle pusher is presently in cylindrical coordinates. However, in the Boris scheme, use is made of a local Cartesian frame to push particles (see Figure 4), and only the aftermath transformation is unique to the individual coordinate system. This scheme is clearly generalizable to any orthogonal system, thus allowing more generality and flexibility in modeling using the MAD3 code.

The most important area of current endeavor is the simulation of space-charge limiting. This phenomenon, described initially in the introduction, results from high levels of x-ray fluence. The important result is a large component of electric field normal to the metallic surface, which diminishes with distance from the surface. However, the high field levels at the surface

tend to inhibit escape of emitted electrons, thus giving rise to a boundary layer with characteristic dimension of centimeters. Because of the spatial variation of the field, resolution would require sub-centimeter spacing; the use of standard techniques is unrealistic in light of such factors as core size and stability criteria.

The approach presently being programmed into MAD3 involves a completely separate one-dimensional steady-state solution (using MAD1) as a function of fluence level ($\tilde{S}$) and external electric field ($\tilde{E}$). The resulting potential is then used as a criterion for the injection of particles, based upon their "one-dimensional energy." This approach is similar in principle to that used in the SEMP code[13], which makes use of a one-dimensional solution of Poisson's equation.[14] An alternate approach involves explicit one-dimensional auxiliary gridding and the retention of low-energy particles in a two-dimensional calculation.[15] Either approach appears applicable to the three-dimensional SGEMP problem.

## SECTION VII

## REFERENCES


1. O. Lopez, "The MUST Code," unpublished report, 1974.

2. B. Goplen, R. Knight, and J. Marks, "Source-Region Electromagnetic Pulse Coupling to Antenna and Cable Structures," Science Applications, Inc., Report, SAI-74-512-AQ, also, AFWL TR-74-337, September 1974.

3. D. E. Mereweather, "Transient Currents Induced on a Metallic Body of Revolution by an Electromagnetic Pulse," IEEE Transactions on Electromagnetic Compatibility, Vol. EMC-13, No. 2, p. 41, May 1971.

4. K. D. Granzow, "Transient Spherical Waves," Journal of Applied Physics, Vol. 39, No. 7, p. 3435, June 1968.

5. J. P. Boris, "Relativistic Plasma Simulation--Optimization of a Hybrid Code," Proceedings of the Fourth Conference on Numerical Simulation of Plasmas, Naval Research Laboratory, p. 3, November 1970.

6. T. A. Dellis and C. J. MacCallum, "QUICKE2: A One-Dimensional Code for Calculating Bulk and Vacuum Emitted Photo-Compton Currents," Sandia Laboratories Report, SLL-74-0218, April 1974.

7. W. L. Chadsey and C. R. Ragona, Proceedings of the National Symposium on Radiation in Space, NASA TM-X2440, p. 786, 1972.

8. W. L. Chadsey and C. W. Wilson, "X-Ray Photoemission," Science Applications, Inc., Report, SAI-75-558-WA, June 1975.

9. A. J. Woods and E. P. Wenaas, "SGEMP Geometry Effects," INTEL-RT 8121-024, presented at IEEE Conference on Nuclear and Space Radiation Effects, July 1975.

REFERENCES (Cont'd)

10. J. Gilbert, personal communication, July 1975.

11. D. L. Mangan and R. A. Perala, "SGEMP Low-Level Simulation of the FLTSATCOM," Mission Research Corporation Report, AMRC-R-49, August 1975.

12. L. Marin, K. S. H. Lee and T. K. Liu, "Analytical Calculations on Photoelectron-Induced Currents on a Model of the FLTSATCOM Satellite," Dikewood Corporation Report, also AFWL TR-75-147, 1975.

13. R. Stettner and H. J. Longley, "Description of the SGEMP Computer Code: SEMP," Mission Research Corporation Report, MRC-R-195, June 1975.

14. D. F. Higgins, "Highly Space Charge Limited SGEMP Calculations," Mission Research Corporation Report, MRC-R-190, June 1975.

15. I. Katz, J. Harvey, and A. Wilson, "Particle Simulation Techniques for SGEMP," Systems, Science and Software Report, SSS-75-R-2604, April 1975.